Letter

Two-dimensional topological Anderson insulator in a HgTe-based semimetal

D. A. Khudaiberdiev,[1] Z. D. Kvon,[2,3] M. S. Ryzhkov,[1] D. A. Kozlov,[4] N. N. Mikhailov,[2] and A. Pimenov[1]
[1]*Institute of Solid State Physics, Vienna University of Technology, 1040 Vienna, Austria*
[2]*Institute of Semiconductor Physics, 630090 Novosibirsk, Russia*
[3]*Department of Physics, Novosibirsk State University, Novosibirsk 630090, Russia*
[4]*Experimental and Applied Physics, University of Regensburg, D-93040 Regensburg, Germany*

(Received 26 April 2024; accepted 8 April 2025; published 9 May 2025)

We report the experimental observation of Anderson localization in two-dimensional (2D) electrons and holes in the bulk of HgTe quantum wells with a semimetallic spectrum and under strong disorder. Surprisingly, the one-dimensional (1D) edge channels, arising from the spectrum's inversion, demonstrate remarkable robustness against disorder due to topological protection. Strong disorder induces a mobility gap in the bulk, enabling access to the 1D edge states and thereby realizing the two-dimensional topological Anderson insulator (TAI) state. Nonlocal transport measurements confirm the emergence of topologically protected edge channels. The TAI state appears to be very sensitive to an external magnetic field applied perpendicular to the sample. The weak magnetic field of 30 mT breaks the topological protection of 1D edge channels, thus turning the system into an ordinary Anderson insulator. At a field of 0.5T, the 2D bulk electrons become delocalized, and the system transforms into a quantum Hall liquid.

DOI: 10.1103/PhysRevResearch.7.L022033

Introduction. Topological insulators (TIs) represent a special state of condensed matter with an insulating bulk and conducting gapless states on the surface or the edge [1–5]. The existence of such materials is justified within a concept of topological ordering, which can be expressed in the form of invariants over the momentum space. In the presence of time-reversal symmetry, materials with band gaps (band insulators) are classified by the topological invariant Z_2 [6], which in the two-dimensional (2D) case can take two values, 1 or 0, thereby providing a distinction between topological and normal insulators. The 2D TI state is sometimes referred to as the quantum spin Hall (QSH) effect [7]. In contrast to the quantum Hall effect (QHE), the formation of the edge states in the QSH effect requires no magnetic field: the spin-up and spin-down electrons propagate along the edge in opposite directions with the time-reversal symmetry being conserved. Experimental evidence of the QSH effect was obtained in HgTe quantum wells (QWs) [8] by demonstration of a resistance plateau around $h/2e^2$ in the longitudinal resistance of a mesoscopic Hall bar. This observation was further confirmed by nonlocal experiments in the ballistic [9] and diffusive [10] transport regimes.

Just after the introduction of the TI state, the existence of topological Anderson insulators (TAIs) was theoretically predicted [11]. The basic idea is that disorder or interaction could transform an ordinary insulator into a 2D TI. The initial prediction inspired intensive theoretical [12–17] research, expanding those ideas into such areas as photonic crystals [18–20], cold atoms [21,22], electronic circuits [23,24], and mechanics [25]. In spite of these efforts, to the best of our knowledge, up to now there has been no experimental confirmation of the original idea of an electronic 2D TAI.

In this Letter, we report experimental observation of a two-dimensional topological Anderson insulator (2D TAI) in a disordered 14 nm HgTe quantum well with a semimetallic spectrum. In HgTe-based semimetals, the 2D bulk conduction and valence bands overlap (∼5 meV for 14 nm QW [26–28]). Therefore, it is usually considered impossible to detect the 2D TI state for these systems, since the bulk states would always shunt the edge. However, the recent observation of Anderson localization for both electrons and holes in this system due to strong disorder [29] opens new possibilities. If the edge states arising from the inverted band structure are topologically protected from Anderson localization, it may be possible to achieve the 2D TI state by increasing disorder. This would localize the 2D bulk states, thus realizing a 2D TAI. It is important to state a fundamental difference to the initial idea of the 2D TAI [11], where the system transforms from an ordinary insulator to the 2D TI as a result of increasing disorder. On the contrary, in the present Letter the bulk state is initially conducting and becomes insulating due to opening of the mobility gap in the disordered state. In our case, the edge states in the clean regime are shunted by the conducting bulk and only start to be observed in the gapped regime due to disorder. Although in both cases disorder is crucial to the emergence of the 2D TI state, we believe that the present approach is even closer to the original idea of Anderson [30].

The investigated samples are Hall-like mesostructures fabricated on the basis of strongly disordered 14 nm HgTe (013) QWs grown by molecular-beam epitaxy. A dielectric layer (200 nm of SiO_2) was deposited on the sample and then covered by a TiAu gate. The schematic cross section of the

Published by the American Physical Society under the terms of the Creative Commons Attribution 4.0 International license. Further distribution of this work must maintain attribution to the author(s) and the published article's title, journal citation, and DOI.

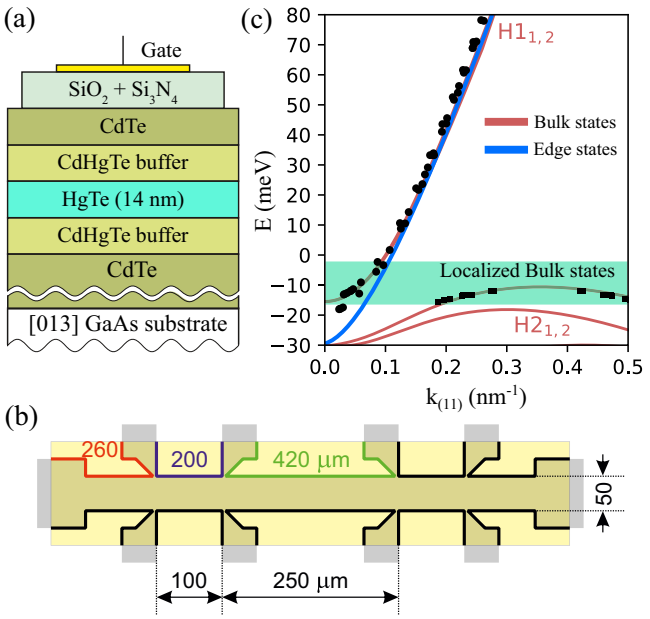


FIG. 1. (a) Cross section of the studied structure. (b) Schematic top view of the Hall bars with the gate (yellow). (c) Energy spectrum of the studied system adapted from Ref. [26]. Red lines are the $\boldsymbol{k \cdot p}$ calculations of the bulk 2D spectrum, with the black dots as the experimentally reconstructed spectrum by the cyclotron-resonance measurements. The turquoise strip represents a mobility gap of the 2D bulk spectrum caused by the Anderson localization. Blue line is an expected topologically protected 1D edge channel spectrum.

QWs is shown in Fig. 1(a), and the sketch of the Hall bar with the gate is given in Fig. 1(b). The measurements were carried out using the standard phase-detecting technique at temperatures of 80 mK–10 K and in magnetic fields up to 1.5 T. The oscillator frequency was in the range 0.3–6 Hz and the driving currents were 1 pA–10 nA depending on the measurement conditions.

Semimetallic state. The energy spectrum of such QWs was reconstructed by the THz spectroscopy technique [26], which agreed with the $\boldsymbol{k \cdot p}$ calculated spectrum. The spectrum from Ref. [26] is adapted to Fig. 1(c). According to these results, the 14 nm HgTe quantum well is a semimetal with a conduction and valence band overlap of about 5 meV.

The system exhibits either purely electronic or semimetallic states depending on the gate voltage (V_g). The gate voltage dependencies of electron (N_s) and hole (P_s) densities at the temperature of $T = 4$ K, determined through Drude fitting of magnetotransport measurements, are shown in Fig. 2(e). An example of semimetallic magnetotransport behavior is provided in the inset. The difference $N_s - P_s$ varies linearly with the gate voltage, crossing zero at the charge neutrality point (CNP) with $V_g^{\mathrm{CNP}} = -0.62$ V. Due to the semimetallic nature of the system, the charge densities at the CNP are nonzero, with $N_s = P_s \approx 2 \times 10^{10}$ cm^{-2}, and to the left from the CNP the system is in the deep semimetallic regime with $N_s \ll P_s$. Notably, the semimetallic state persists down to the base temperature of $T \approx 80$ mK for strongly negative gate voltages. This is evidenced by the sign-alternating Hall resistivity, as shown in Fig. 2(f). These results demonstrate that the overlap between the conduction and valence bands is maintained across the entire temperature range, confirming the absence of a band gap in the studied system.

2D TAI in nonlocal transport. The observation of both local (R_{loc}) and nonlocal (R_{nonloc}) resistances in the absence of magnetic field is generally considered [9,10] a direct indication of a 2D TI state. In that case, the current flows through the sample along its edges, and a measurable resistance $R \propto V (I = \mathrm{const})$ exists regardless of the positions of the voltage probes with respect to the current contacts. Figure 2 presents the results of the resistance measurements in local and nonlocal configurations. Figures 2(a)–2(c) show the gate-voltage dependencies of R_{loc}, R_{nonloc}, and $R_{\mathrm{nonloc}}^{\mathrm{far}}$, respectively. At first glance, qualitatively similar behavior of local and nonlocal resistances is observed: both exhibit a broad maximum ($V_g^{\max} = -0.74$ V), slightly shifted to negative voltages from the CNP, followed by a sharp decrease on either side of the curve. The detailed analysis of the data reveals the fundamental difference between local and nonlocal resistances: First, the maximum plateau in $R_{\mathrm{loc}}(V_g)$ is notably wider than that in $R_{\mathrm{nonloc}}(V_g)$ and $R_{\mathrm{nonloc}}^{\mathrm{far}}(V_g)$, and, second, both nonlocal responses vanish for increasing temperatures while the local one remains finite up to the highest temperatures. Figure 2(d) shows all three resistances as the function of temperature at $V_g = V_g^{\max}$. For high temperatures above $\sim$1 K, all resistances increase exponentially as the temperature decreases. The activation energy for the local resistance is 1.7 meV (the exponential slope is indicated by dash-dotted green line). For temperatures $T > 0.4$ K, the condition $R_{\mathrm{loc}} \gg R_{\mathrm{nonloc}}, R_{\mathrm{nonloc}}^{\mathrm{far}}$ holds, indicating that the transport mechanism is dominated by the bulk. At lower temperatures $T \lesssim 0.5$ K, the resistance increase slows down and eventually saturates. In this regime, both R_{nonloc} and $R_{\mathrm{nonloc}}^{\mathrm{far}}$ become comparable to or even exceed R_{loc}, reflecting a transition to a transport mechanism dominated by edge contributions.

The observed behavior of local and nonlocal responses is typical for the 2D TI, as it follows from the fundamental difference in the relative contributions of the bulk and edge conductivities for local and nonlocal configurations [9,31–34]. At high temperatures, the bulk contribution dominates, resulting in nonlocal resistances being exponentially smaller than the local one. As the temperature decreases, particularly in the presence of strong disorder, the bulk contribution to transport diminishes exponentially due to localization effects. Consequently, nonlocal transport along the sample edges becomes the dominant mechanism. In this regime, the ratio of voltages or resistances measured in local and nonlocal configurations is governed by the currents flowing along the sample edges and the positioning of the voltage probes. In the extreme case where current flows exclusively along the sample edges, the geometry of the sample causes the voltage drop in the local configuration to become smaller than the one in the nonlocal configuration. In the extreme regime where the current flows solely along the sample edges, due to the geometry of the sample the voltage drop in the local configuration is even lower than the ones in nonlocal. In addition, for $T < 0.2$ K and for all investigated configurations, the resistance maximum $R_{\mathrm{nonloc}}(V_g)$ is more than two orders of magnitude larger than h/e^2, thus indicating that the edge

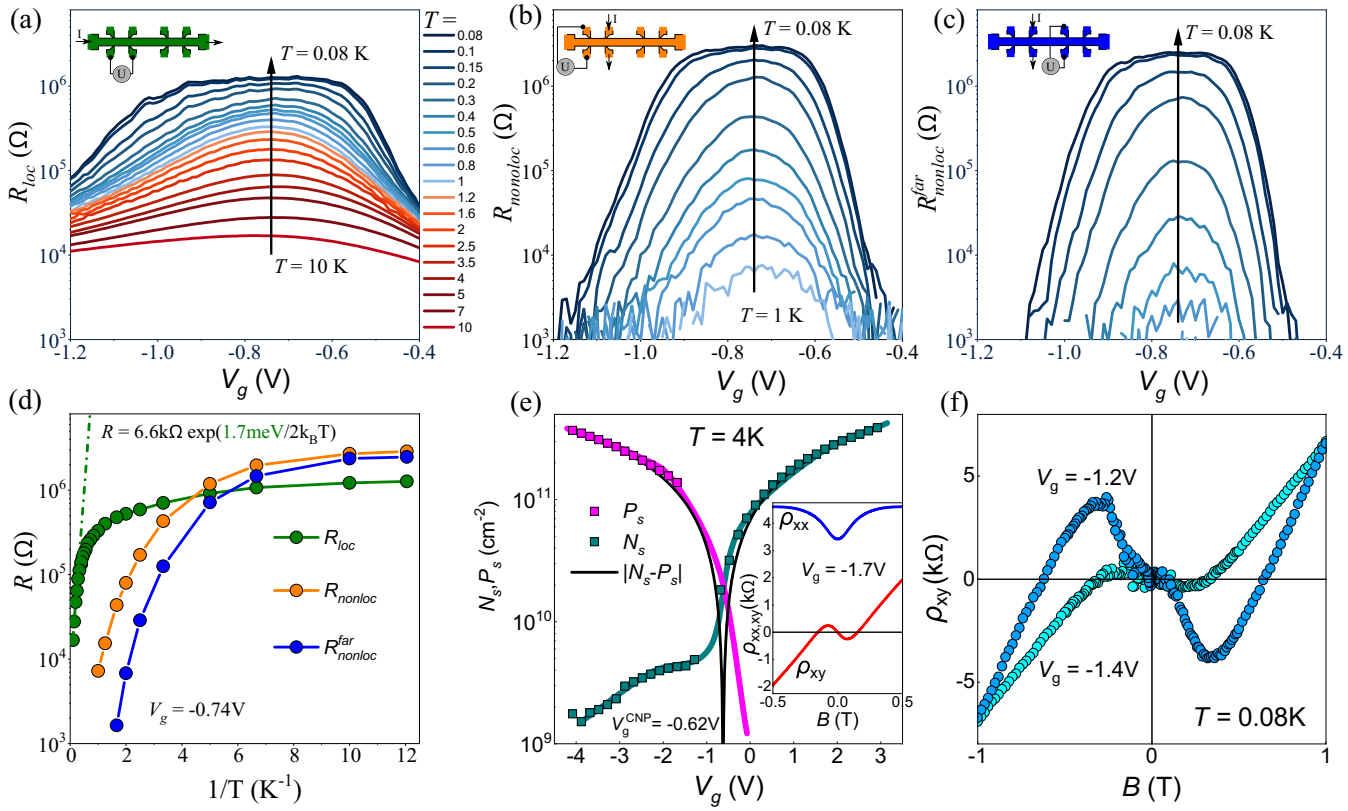


FIG. 2. (a) Local, (b) nonlocal, and (c) far nonlocal resistances as functions of the gate voltage (V_g) at various temperatures (the legend is valid for all three graphs). (d) Local and both nonlocal resistances plotted as functions of the inverse temperature at $V_g = -0.74$ V corresponding to the resistance maxima, as indicated by arrows in (a)–(c). (e) Gate-voltage dependence of the electron (N_s, pink squares) and hole (P_s, dark cyan squares) concentrations extracted using the two-component Drude model. The inset shows an example of the fitted data. Corresponding colored lines guide the eye. The black line represents the absolute difference $|N_s - P_s|$, highlighting the charge neutrality point ($V_g^{\mathrm{CNP}} = -0.62$ V). (f) Magnetic-field dependence of the Hall resistance ρ_{xy} at the base temperature for $V_g = -1.2$ V (dark blue) and $V_g = -1.4$ V (cyan).

transport is diffusive with mean free path $l_{\mathrm{edge}} \approx 1$ μm. This value is quite typical for disordered 2D TI [8,10,31]. Although scattering occurs within the 1D edge channels, topological protection prevents the complete localization of these states, contrary to predictions from conventional scaling theory [35]. The 1D conductivity scaling under topological protection is rather classical with only incoherent scattering. However, breaking time-reversal symmetry (see Fig. 3) restores conventional localization mechanisms [36].

The described relation between 2D bulk and 1D edge states of 2D TI with respect to Anderson localization represent the main result of the this Letter. While 2D bulk electrons and holes are strongly localized with an exponential temperature dependence of resistance, the 1D edge current states experience no Anderson localization due to topological protection and continue to conduct even at the lowest temperatures. This finding emphasizes an incredible robustness of the topologically protected edge channels, which survived under strong disorder even when the bulk states were localized. The fact that the 2D TI state is only achievable due to Anderson localization indicates that we are dealing with another kind of 2D TI–2D topological Anderson insulator with a 2D band of the localized states and 1D conducting states.

Further on, one might notice that in the vicinity of the CNP and for $T < 0.2$ K, gate-voltage dependencies of all resistances are rather weak [see Figs. 2(a)–2(c)]. In this regime where the edge transport dominates, the maxima are wide, such that the resistance does not change in the broad voltage range of around 0.3 V. This behavior significantly differs from the one observed in narrow gap 2D TI [31], where a quite sharp resistance peak is observed and both $R_{\mathrm{loc}}(V_g)$ and $R_{\mathrm{nonloc}}(V_g)$ are strongly asymmetrical with respect to the maximum position. We suggest the following explanation for this observation, taking into account the energy spectrum—the 2D topological Anderson insulator given in Fig. 1(c). The conduction (H1) and valence (H2) bands [Fig. 1(c)] in our system are mostly formed by the Γ_8 band, while the Γ_6 band state E1 is pushed deep into the energy spectrum [37]. This implies that the Dirac point of the edge states is also deep inside the valence band, thus in an experimentally accessible gate range the Fermi level remains always in the electron part of the edge spectrum. This regime roughly corresponds to the turquoise area in the band spectrum shown in Fig. 1(c). In the regime of localized bulk states and the edge spectrum far from the Dirac point, the maximum of resistivity in the edge transport regime is wide and nearly symmetric.

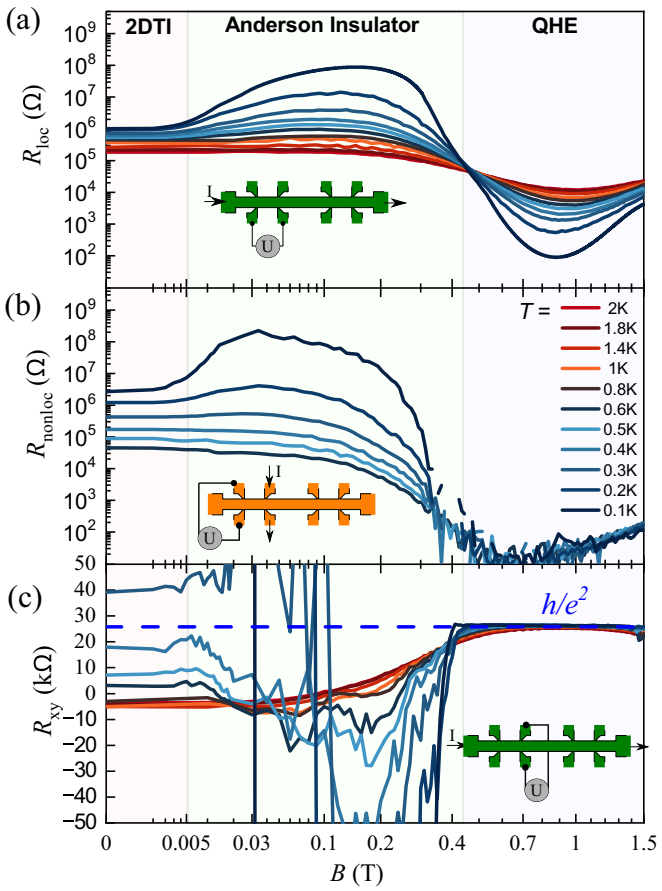


FIG. 3. Magnetoresistance of a topological Anderson insulator. (a) Local, (b) nonlocal, and (c) Hall resistances at $V_g = -0.74$ V in the temperature range from 100 mK to 2 K. The magnetic field axis is scaled as the cube root to emphasize both 2D TI-to-Anderson insulator and Anderson insulator-to-quantum Hall liquid transitions.

Phase transitions under perpendicular magnetic field. To further investigate the 2D TAI state, we performed the magnetotransport measurements (magnetic field is perpendicular to the sample's plane) at the gate voltage $V_g = V_g^{\max}$. The magnetic field dependencies of the local $R_{\rm loc}(B)$, nonlocal $R_{\rm nonloc}(B)$, and Hall $R_{xy}(B)$ resistances are shown in Fig. 3. We identify three transport regimes of the system depending on the applied magnetic field: 2D TI, ordinary Anderson insulator, and the quantum Hall liquid.

At zero magnetic field, the system is in the 2D TI state, as discussed above. At low temperatures $R_{\rm loc} \ll R_{\rm nonloc}$, which indicates that the transport is going predominantly along the sample's edges. The low-temperature Hall resistance R_{xy} takes random values due to possible asymmetry of the top and bottom paths of the electrons along the edges, but it is still orders of magnitude smaller than both local and nonlocal resistances.

Then, at low magnetic fields between 5 mT and 200 mT, we observe the breakdown of 2D TI topological protection, which leads the system into the (ordinary) Anderson insulator regime with the mobility gap preventing the current flow. Both $R_{\rm nonloc}$ and $R_{\rm loc}$ grow by about two orders of magnitude, exceeding the values of 100 MΩ. Compared to the field-free regime, the edge states are not topologically protected due to the breaking of time-reversal symmetry and the magnetic field-induced helical edge-state localization. This effect is similar to the one observed in 8 nm HgTe QWs [36] without strong disorder. Observed time-reversal symmetry breaking supports the 2D TAI picture.

Finally, in high magnetic fields, the system is in the quantum Hall liquid state. As one can see in both $R_{\rm loc}$ and R_{xy}, there is a quantum phase transition from Anderson insulator to the quantum Hall liquid [38–40] at a critical magnetic field of $B_c \approx 0.5$ T and with critical resistance $\rho_{xx}(B_c) \approx 1.5\ h/e^2$. It is worth noting that compared to the results on GaAs-based QWs [38,39], the transition in our case occurs at much lower (almost one order of magnitude) magnetic fields and the filling factor ν is 1 rather than 2. It is not surprising because the 2D electrons in HgTe QWs have completely different Landau level spectrum with larger cyclotron gap, large Zeeman splitting ($g\mu_B > \hbar\omega_c/2$), and because the two-component electron-hole system is affected by Anderson localization [29]. The holes are apparently still localized and do not contribute to the Hall conductivity, allowing perfect quantization.

A transition from an ordinary 2D TI with the bulk gap to the quantum Hall state was predicted theoretically [41,42] and studied experimentally [43,44]. It is necessary to note that in these works the bulk was characterized by a band gap contrasted to the mobility gap due to disorder in our case.

Conclusion. In this Letter, we investigated a 14-nm-wide HgTe quantum well with a semimetallic energy spectrum. Our findings reveal that in the presence of disorder, the 2D bulk electrons and holes exhibit strong Anderson localization, but at the same time the topologically protected 1D edge current states, emerging from the inversion of the spectrum, remain unaffected. This underscores the robustness of the topologically protected 1D edge channels and their dominance over the 2D bulk states, in stark contrast to the predictions of scaling theory, which suggests that 1D transport should be more vulnerable than 2D transport. As a result, we demonstrate the realization of another type of 2D topological insulator—a 2D topological Anderson insulator with a localized bulk band. Furthermore, in the presence of perpendicular magnetic field we observe two quantum phase transitions. An external field as small as 30 mT is enough to break the topological protection and to localize the 1D edge channels, which leads to an ordinary Anderson insulator state. In higher fields above 0.5 T, we observe the transition from the Anderson insulator to the quantum Hall liquid. These transitions raise a fundamental question of how the helical edge states in 2D TI are transformed into the chiral edge states of the QHE.

Acknowledgments. The authors acknowledge the TU Wien Bibliothek for financial support through its Open Access Funding Programme and the Russian Science Foundation (Grant No. 23-72-30003).

[1] M. Z. Hasan and C. L. Kane, *Colloquium*: Topological insulators, Rev. Mod. Phys. **82**, 3045 (2010).

[2] X.-L. Qi and S.-C. Zhang, Topological insulators and superconductors, Rev. Mod. Phys. **83**, 1057 (2011).

[3] X.-L. Qi and S.-C. Zhang, The quantum spin Hall effect and topological insulators, Phys. Today **63** (1), 33 (2010).

[4] J. E. Moore and L. Balents, Topological invariants of time-reversal-invariant band structures, Phys. Rev. B **75**, 121306(R) (2007)

[5] J. E. Moore, The birth of topological insulators, Nature (London) **464**, 194 (2010).

[6] C. Kane and E. Mele, Z_2 topological order and the quantum spin Hall effect, Phys. Rev. Lett. **95**, 146802 (2005).

[7] B. A. Bernevig, T. L. Hughes, and S.-C. Zhang, Quantum spin Hall effect and topological phase transition in HgTe quantum wells, Science **314**, 1757 (2006).

[8] M. König, S. Wiedmann, C. Brüne, A. Roth, H. Buhmann, L. W. Molenkamp, X.-L. Qi, and S.-C. Zhang, Quantum spin Hall insulator state in HgTe quantum wells, Science **318**, 766 (2007).

[9] A. Roth, C. Brüne, H. Buhmann, L. W. Molenkamp, J. Maciejko, X.-L. Qi, and S.-C. Zhang, Nonlocal transport in the quantum spin Hall state, Science **325**, 294 (2009).

[10] G. M. Gusev, Z. D. Kvon, O. A. Shegai, N. N. Mikhailov, S. A. Dvoretsky, and J. Portal, Transport in disordered two-dimensional topological insulators, Phys. Rev. B **84**, 121302(R) (2011).

[11] J. Li, R. L. Chu, J. K. Jain, and S. Q. Shen, Topological Anderson insulator, Phys. Rev. Lett. **102**, 136806 (2009).

[12] H. Jiang, Lei Wang, Q.-F. Sun, and X. C. Xie, Numerical study of the topological Anderson insulator in HgTe/CdTe quantum wells, Phys. Rev. B **80**, 165316 (2009).

[13] C. W. Groth, M. Wimmer, A. R. Akhmerov, J. Tworzydło, and C. W. J. Beenakker, Theory of the topological Anderson insulator, Phys. Rev. Lett. **103**, 196805 (2009).

[14] Y. Xing, L. Zhang, and J. Wang, Topological Anderson insulator phenomena, Phys. Rev. B **84**, 035110 (2011).

[15] R. Chen, D.-H. Xu, and B. Zhou, Topological Anderson insulator phase in a Dirac-semimetal thin film, Phys. Rev. B **95**, 245305 (2017).

[16] D. D. Vu and S. Das Sarma, Weak quantization of noninteracting topological Anderson insulator, Phys. Rev. B **106**, 134201 (2022).

[17] B. D. Assunção, G. J. Ferreira, and C. H. Lewenkopf, Phase transitions and scale invariance in topological Anderson insulators, Phys. Rev. B **109**, L201102 (2024).

[18] S. Stützer, Y. Plotnik, Y. Lumer, P. Titum, N. H. Lindner, M. Segev, M. C. Rechtsman, and A. Szameit, Photonic topological Anderson insulators, Nature (London) **560**, 461 (2018).

[19] G.-G. Liu, Y. Yang, X. Ren, H. Xue, X. Lin, Y.-H. Hu, H.-X. Sun, B. Peng, P. Zhou, Y. Chong, and B. Zhang, Topological Anderson insulator in disordered photonic crystals, Phys. Rev. Lett. **125**, 133603 (2020).

[20] M. Ren, Y. Yu, B. Wu, X. Qi, Y. Wang, X. Yao, J. Ren, Z. Guo, H. Jiang, H. Chen, X.-J. Liu, Z. Chen, and Y. Sun, Realization of gapped and ungapped photonic topological Anderson insulators, Phys. Rev. Lett. **132**, 066602 (2024).

[21] E. J. Meier, F. A. An, A. Dauphin, M. Meffei, P. Massignan, T. L. Hughes, and B. Gadway, Observation of the topological Anderson insulator in disordered atomic wires, Science **362**, 929 (2018).

[22] S. Nakajima, N. Takei, K. Sakuma, Y. Kuno, P. Marra, and Y. Takahashi, Competition and interplay between topology and quasi-periodic disorder in Thouless pumping of ultracold atoms, Nat. Phys. **17**, 844 (2021).

[23] Z. Q. Zhang, B. L. Wu, J. Song, and H. Jiang, Topological Anderson insulator in electric circuits, Phys. Rev. B **100**, 184202 (2019).

[24] W. Zhang, D. Zou, Q. Pei, W. He, J. Bao, H. Sun, and X. Zhang, Experimental observation of higher-order topological Anderson insulators, Phys. Rev. Lett. **126**, 146802 (2021).

[25] X. Shi, I. Kiorpelidis, R. Chaunsali, V. Achilleos, G. Theocharis, and J. Yang, Disorder-induced topological phase transition in a one-dimensional mechanical system, Phys. Rev. Res. **3**, 033012 (2021).

[26] J. Gospodarič, A. Shuvaev, N. N. Mikhailov, Z. D. Kvon, E. G. Novik, and A. Pimenov, Energy spectrum of semimetallic HgTe quantum wells, Phys. Rev. B **104**, 115307 (2021).

[27] N. N. Vasil'ev, Z. D. Kvon, N. N. Mikhailov, and S. D. Ganichev, Two-Dimensional semimetal HgTe in 14-nm-thick quantum wells, JETP Lett. **113**, 466 (2021).

[28] D. Khudaiberdiev, Z. D. Kvon, M. V. Entin, D. A. Kozlov, N. N. Mikhailov, and M. Ryzhkov, Mesoscopic conductance fluctuations in 2D HgTe semimetal, Nanomaterials **13**, 2882 (2023).

[29] Z. D. Kvon, E. B. Olshanetsky, M. A. Drofa, and N. N. Mikhailov, Anderson localization in a two-dimensional electron-hole system, JETP Lett. **114**, 341 (2021).

[30] P. W. Anderson, Absence of diffusion in certain random lattices, Phys. Rev. **109**, 1492 (1958).

[31] E. B. Olshanetsky, Z. D. Kvon, G. M. Gusev, A. D. Levin, O. E. Raichev, N. N. Mikhailov, and S. A. Dvoretsky, Persistence of a two-dimensional topological insulator state in wide HgTe quantum wells, Phys. Rev. Lett. **114**, 126802 (2015).

[32] Z. D. Kvon, D. A. Kozlov, E. B. Olshanetsky, G. M. Gusev, N. N. Mikhailov, and S. A. Dvoretsky, Topological insulators based on HgTe, Usp. Fiz. Nauk. **190**, 673 (2020).

[33] S. Benlenqwanssa, S. S. Krishtopenko, M. Meyer, B. Benhamou-Bui, L. Bonnet, A. Wolf, C. Bray, C. Consejo, S. Ruffenach, S. Nanot, J.-B. Rodriguez, E. Tourni, F. Hartmann, S. Höfling, F. Teppe, and B. Jouault, Multi-probe analysis to separate edge currents from bulk currents in quantum spin Hall insulators and to analyze their temperature dependence, Phys. Rev. Appl. **22**, 064059, (2024).

[34] G. M. Gusev, Z. D. Kvon, E. B. Olshanetsky, A. D. Levin, Y. Krupko, J. C. Portal, N. N. Mikhailov, and S. A. Dvoretsky, Temperature dependence of the resistance of a two-dimensional topological insulator in a HgTe quantum well, Phys. Rev. B **89**, 125305 (2014).

[35] E. Abrahams, P. W. Anderson, D. C. Licciardello, and T. V. Ramakrishnan, Scaling theory of localization: Absence of quantum diffusion in two dimensions, Phys. Rev. Lett. **42**, 673 (1979).

[36] S. U. Piatrusha, E. S. Tikhonov, Z. D. Kvon, N. N. Mikhailov, S. A. Dvoretsky, and V. S. Khrapai, Topological protection brought to light by the time-reversal symmetry breaking, Phys. Rev. Lett. **123**, 056801 (2019).

[37] M. König, H. Buhmann, L. W. Molenkamp, T. Huges, C. X. Liu, X. L. Qi, and S.-C. Zhang, The quantum spin Hall effect: Theory and experiment, J. Phys. Soc. Jpn. **77**, 031007 (2008).

[38] H. W. Jiang, C. E. Johnson, K. L. Wang, and S. T. Hannahs, Observation of magnetic-field-induced delocalization: Transi-

tion from Anderson insulator to quantum Hall conductor, Phys. Rev. Lett. **71**, 1439 (1993).

[39] R. J. Hughes, J. T. Nicholls, J. E. Frost, E. H. Linfield, M. Pepper, C. J. Ford, D. A. Ritchie, G. A. Jones, E. Kogan, and M. Kaveh, Magnetic-field-induced insulator-quantum Hall-insulator transition in a disordered two-dimensional electron gas, J. Phys.: Condens. Matter **6**, 4763 (1994).

[40] D. Shahar, D. C. Tsui, and J. E. Cunningham, Observation of the $\nu = 1$ quantum Hall effect in a strongly localized two-dimensional system, Phys. Rev. B **52**, R14372(R) (1995).

[41] B. Scharf, A. Matos-Abiague, and J. Fabian, Magnetic properties of HgTe quantum wells, Phys. Rev. B **86**, 075418 (2012).

[42] M. V. Durnev and S. A. Tarasenko, Magnetic field effects on edge and bulk states in topological insulators based on HgTe/CdHgTe quantum wells with strong natural interface inversion asymmetry, Phys. Rev. B **93**, 075434 (2016).

[43] E. B. Olshanetsky, Z. D. Kvon, G. M. Gusev, N. N. Mikhailov, and S. A. Dvoretsky, Two dimensional topological insulator in quantizing magnetic fields, Physica E **99**, 335 (2018).

[44] S. Shamim, P. Shekhar, W. Beugeling, J. Böttcher, A. Budewitz, J. B. Mayer, L. Lunczer, E. M. Hankiewicz, H. Buhmann, and L. W. Molenkamp, Counterpropagating topological and quantum Hall edge channels, Nat. Commun. **13**, 2682 (2022).